Detection of biomolecular microarrays without fluorescent-labeling agents

J. P. Landry[a], X. D. Zhu[a], J. P. Gregg[b], X. W. Guo[c]
[a]Dept. of Physics, NSF Center for Biophotonics Science & Technology, University of California at Davis, One Shields Avenue, Davis, CA 95616
[b]Dept. of Pathology, UCD School of Medicine, 4645 Second Ave., Sacramento, CA 95817
[c]Bio-Rad Laboratories Inc., 3148 Industry Boulevard, West Sacramento, CA 95691

ABSTRACT

We developed an optical oblique-incidence reflectivity difference (OI-RD) scanning microscope for imaging microarrays of label-free protein and DNA. Such a microscope complements currently widely used fluorescence-based optical microscopes by offering the capability to detect biochemical activities of DNA and protein molecules without the influence of fluorescent-labeling molecules. The specific activity and function of protein molecules are particularly subject to binding of small or large foreign molecules either directly through conformational change in the protein molecule itself or indirectly through properties of the attached molecules. We show that an OI-RD microscope can be used to: 1) detect binding reactions on microarrays *without labeling*, 2) quantitatively measure the optical properties of microarray spots, and 3) detect microarrays submerged in solution (which will enable OI-RD to monitor reaction kinetics on microarrays in reactive solutions). Furthermore, using both OI-RD and fluorescence images of an immunoglobulin-G (IgG) protein microarray, we observed that labeled and unlabeled IgG molecules deposited on the microarray substrate exhibit different wetting behaviors, and a mixture of the two tends to segregate into labeled and unlabeled regions. This illustrates potentially undesirable effects of fluorescent-labeling agents on protein properties that are of interest.

Keywords: microarrays, biochips, label-free detection, in-situ detection, ellipsometry, oblique-incidence reflectivity difference, OI-RD, hybridization, oligonucleotide, immunoglobulin-G

1. INTRODUCTION

Microarrays are micron-scale spots of immobilized biomolecules (such as DNA or protein) arranged in a regular pattern on a solid substrate (typically glass)[1]. Due to their inherent high spot density, microarrays enable thousands of biomolecular interactions to be investigated in a parallel fashion. Microarrays are typically reacted with fluorophore-labeled probe molecules and subsequently detected using fluorescence microscopes. Fluorescence labeling has been very successful for detecting nucleic acid interactions on microarrays. One reason for this is that the structure and reactivity of nucleic acids are relatively uniform and minimally affected by fluorophore molecules. However, this is not the case for proteins. There is now vigorous activity in the development of protein microarrays for high-throughput quantitative and functional proteomics[2]. Because the structure and reactivity of proteins are much more complex and diverse than DNA, the attachment of a fluorophore to a protein may change how the protein binds to other molecules[2]. Furthermore, the efficiency of labeling may vary from protein to protein making it difficult to measure the relative abundances of a set of unrelated proteins[3]. *Label-free detection of reactions on microarrays circumvents these problems.*

In this paper we show that an optical *oblique-incidence reflectivity difference* (OI-RD) microscope can be used to: 1) detect binding reactions on microarrays without labeling, 2) quantitatively measure the optical properties of microarray spots, and 3) detect microarrays submerged in solution (which will enable OI-RD to monitor reaction kinetics on microarrays in reactive solutions). Furthermore, the potentially undesirable impact labeling can have upon the physical properties of proteins is demonstrated using fluorescence and OI-RD images of immunoglobulin-G (IgG) protein microarrays.

Microarrays and Combinatorial Techniques: Design, Fabrication, and Analysis II,
edited by Dan V. Nicolau, Ramesh Raghavachari, Proceedings of SPIE Vol. 5328
(SPIE, Bellingham, WA, 2004) · 1605-7422/04/$15 · doi: 10.1117/12.524554

2. INSTRUMENT

OI-RD is a particular form of optical ellipsometry that measures optical properties of a thin film on a surface[4,5]. At oblique incidence, the reflectivities for *p*- and *s*-polarized light change disproportionately in response to such a film. Let r_{p0} and r_{s0} be the reflectivities from the bare surface, r_p and r_s be the reflectivities from the surface covered with a thin film, and we define $\Delta_p = (r_p - r_{p0})/r_{p0}$ and $\Delta_s = (r_s - r_{s0})/r_{s0}$. In the limit that the film thickness d is much less than the optical wavelength λ, the OI-RD technique enables direct measurements of the real and imaginary parts of $\Delta_p - \Delta_s$. In terms of the ellipsometric ratio[6] $\rho = r_p/r_s = \tan\psi \exp(i\delta)$, it is easily seen that $\Delta_p - \Delta_s \approx (\rho - \rho_0)/\rho_0$, so that $\mathrm{Im}\{\Delta_p - \Delta_s\} \approx \delta - \delta_0$, and $\mathrm{Re}\{\Delta_p - \Delta_s\} \approx 2\csc\psi_0\,(\psi - \psi_0)$.

The layout of our OI-RD microscope is shown in Fig. 1a. A *p*-polarized He-Ne laser beam with $\lambda = 632$ nm passes through a photoelastic modulator (modulation frequency $\Omega = 50$ kHz, maximum retardation of 180°, modulation axis at 45° relative to *p*-polarization). The modulator causes the output beam to oscillate between *p*- and *s*-polarization, with elliptically polarized intermediate states. The polarization-modulated beam then passes through a Pockels cell that introduces an adjustable phase ϕ_0 between the *s*- and *p*-polarized components. The resultant beam is focused to a ~5 μm spot on a microarray-containing surface at an incidence angle θ. After reflection and re-collimation, the beam passes through an analyzer. The intensity of the transmitted beam $I_R(t)$ is detected with a photodiode and Fourier analyzed with digital lock-in amplifiers. $I_R(t)$ consists of various harmonics of the modulation frequency Ω. We detect the first and second harmonic amplitudes, $I(\Omega)$ and $I(2\Omega)$. Initially the sample is moved to a position where the incident beam reflects off the bare surface. We adjust the analyzer to zero $I(2\Omega)$ and then adjust the phase ϕ_0 (with the Pockels cell) to zero $I(\Omega)$. During the subsequent scan over regions of the surface with features of the microarray, $I(\Omega) \sim \mathrm{Im}\{\Delta_p - \Delta_s\}$ and $I(2\Omega) \sim \mathrm{Re}\{\Delta_p - \Delta_s\}$. The proportionality constants are measured separately so that $\Delta_p - \Delta_s$ is determined absolutely[7]. In the present study, we only record $\mathrm{Im}\{\Delta_p - \Delta_s\}$ images by moving the sample underneath the fixed optics.

Microarrays printed on transparent substrates can be scanned in one of two configurations. Dry microarrays are scanned by reflecting the laser directly from the microarray-containing surface as shown in Fig 1a. For this configuration, it has been shown[4] that

$$\Delta_p - \Delta_s \approx -i\left[\frac{4\pi\varepsilon_s \sin^2\theta\cos\theta}{(\varepsilon_s - 1)(\varepsilon_s\cos^2\theta - \sin^2\theta)}\right]\frac{(\varepsilon_d - \varepsilon_s)(\varepsilon_d - 1)}{\varepsilon_d}\left(\frac{d}{\lambda}\right). \quad (1)$$

θ is the angle of incidence while ε_d and ε_s are the optical dielectric constants for the film and the substrate, respectively, at the wavelength λ. To scan microarrays immersed in a reactive solution, the substrate is used as a window to a reaction chamber as shown in Fig 1b. In this configuration

$$\Delta_p - \Delta_s \approx -i\left[\frac{4\pi\varepsilon_s^{1/2}\varepsilon_0 \sin^2\theta\cos\theta}{(\varepsilon_0 - \varepsilon_s)(\varepsilon_0\cos^2\theta - \varepsilon_s\sin^2\theta)}\right]\frac{(\varepsilon_d - \varepsilon_s)(\varepsilon_d - \varepsilon_0)}{\varepsilon_d}\left(\frac{d}{\lambda}\right). \quad (2)$$

θ is the angle of incidence at the microarray-containing surface while ε_0, ε_d, and ε_s are the optical dielectric constants for the ambient, the film, and the substrate, respectively, at the wavelength λ. At He-Ne laser wavelength of 632.8 nm, $\varepsilon_0 = 1$ (air) or $\varepsilon_0 = 1.77$ (water), $\varepsilon_s = 2.31$ (glass slide), and ε_d is real for a film of unlabeled DNA or IgG. As a result, only $\mathrm{Im}\{\Delta_p - \Delta_s\}$ is non-zero in either configuration.

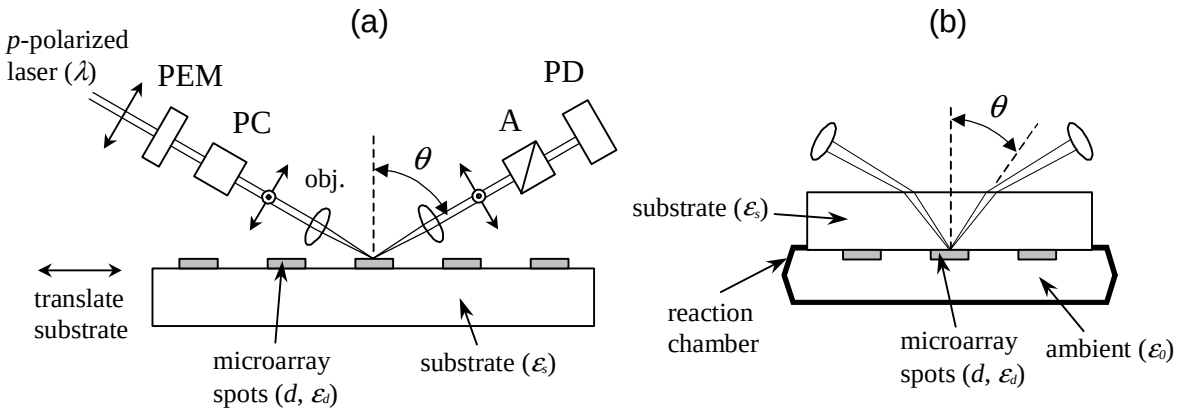

Fig. 1 Optical arrangement of an oblique-incidence reflectivity difference (OI-RD) scanning microscope for microarray imaging. The substrate (and reaction chamber, if present) is on a pair of translation stages that are movable along x and y directions. Dry microarrays are imaged as shown in (a), while microarrays immersed in solution are imaged as shown in (b). PEM: photoelastic modulator; PC: Pockels cell; obj: objective; A: analyzer; PD: photodiode.

3. MICROARRAY PROCESSING

3.1. Oligonucleotide microarrays

The oligonucleotide microarrays were fabricated using a "pin-and-ring" contact-printing robot (Genetic Microsystems GMS 417). The printing pin diameter was 125 µm and the volume of the deposited solution was about 1 nL. 60-base oligonucleotides (Sigma-Genosys) in ultra-pure nuclease-free water were printed on poly-L-lysine coated glass slides (CEL Associates). At neutral pH, negatively charged oligonucleotides bind electrostatically to positively charged amino groups on the poly-L-lysine coated slide[8]. After printing, the microarrays were irradiated with UV light (λ = 254 nm) at a dosage of either 60 mJ/cm^2 or 600 mJ/cm^2 to induce covalent bonds[9]. Excess oligonucleotides were washed off by immersing the printed glass slide in sodium borate buffer (pH 8.5) for 4 minutes. The remaining amino groups on the glass slide were blocked with succinic anhydride in borate-buffered 1-methyl-2-pyrolidinone for one hour[9]. Hybridization reactions were performed in a mixture of 3× saline sodium citrate (SSC), 0.2% sodium dodecyl sulfate (SDS) and 2 µM 60-base oligonucleotide probe at 25°C for 1 hour. The probe concentration was high enough to ensure complete hybridization between the complementary probe and the printed oligonucleotides. After the reaction, the microarray was rinsed in 2×SSC / 0.25% SDS for 2 minutes, then 0.2×SSC for 2 minutes, and finally ddH_2O for 2 minutes. Images of "dry microarrays" were obtained after drying the slide by centrifugation and letting them sit overnight in a slide box. Cy5 fluorescence images were acquired with a confocal fluorescence scanner (Genetic Microsystems GMS 418).

3.2. IgG microarrays

Unlabeled, Cy3 labeled, and Cy5 labeled whole IgG monoclonal antibodies (Jackson Immuno Research) were printed on aldehyde-derivatized glass slides (CEL Associates) using the same printing robot as the oligonucleotide microarrays. Spectrophotometric measurements of the nominally labeled IgG solutions (in 1× phosphate buffered saline (PBS)) yielded dye-to-protein ratios of ~0.5, indicating that about half of the IgG in the solution was actually unlabeled. The dye-to-protein ratio was computed by measuring the absorbance of the protein at λ = 280 nm and the absorbance of the fluorophore at the excitation peak of the dye (λ = 550 nm for Cy3, λ = 650 nm for Cy5)[10]. For printing, the IgG was mixed in a 40% glycerol, 60% 1×PBS (v/v) solution. The IgG is covalently bound to the substrate through a Schiff base linkage formed by the substrate aldehyde groups and the primary amines of surface lysine residues on the IgG molecule[1]. Excess printed protein was washed off by immersing in ddH_2O for 15 minutes. The remaining aldehyde groups on the glass slide were blocked by immersing in a 1% solution of IgG-free bovine serum albumin (BSA) (Jackson Immuno Research) in 1×PBS for 1 hr. Reactions with secondary antibodies were performed in a mixture of

1% BSA, 1×PBS, and 0.5 µg/ml secondary antibody at 25°C for 30 minutes. After the reaction, the microarray was rinsed in 0.1% TWEEN20 in 1×PBS for 2 minutes, then 1×PBS for 2 minutes, and finally ddH_2O for 2 minutes. Images of "dry microarrays" were obtained after drying the slide by centrifugation and letting them sit overnight in a slide box. Cy5 and Cy3 fluorescence images were acquired using the same fluorescence scanner as before.

4. RESULTS AND ANALYSIS

4.1. OI-RD detection of hybridization reactions on an oligonucleotide microarray

Label-free OI-RD detection of binding reactions on microarrays is demonstrated in Fig. 2. Each image was acquired when the array was dry (as described above) in the configuration shown in Fig. 1a with $\theta = 45^o$. Fig. 2a shows an $\mathrm{Im}\{\Delta_p - \Delta_s\}$ image of an oligonucleotide microarray before hybridization. Each column was printed with unlabeled oligonucleotides of unique sequence, as listed in Table 1. Before imaging, the printed microarray was UV cross-linked (60 mJ/cm^2) and then washed so that excess oligonucleotides on top of a saturated monolayer were removed. In this experiment, the printing concentration was in excess of 40 µM to ensure the saturation condition (see Fig. 3). The top spot in column 3 was left blank for alignment control. The eight spots in this image have roughly equal values of $\mathrm{Im}\{\Delta_p - \Delta_s\}$. Fig. 2b shows the $\mathrm{Im}\{\Delta_p - \Delta_s\}$ image after the microarray is hybridized with a solution of unlabeled oligonucleotides complementary to column 1 and Cy5-labeled oligonucleotides complementary to column 3. Column 2 was not reacted for quality control. Fig. 2c shows a Cy5-fluorescence image of the microarray after the hybridization, revealing the two hybridized spots in column 3. This image confirms that the solution-phase oligonucleotides bound only to the complementary oligonucleotides that were printed on the glass slide. Fig. 2d shows the differential $\mathrm{Im}\{\Delta_p - \Delta_s\}$ image obtained by subtracting Fig. 2a from Fig. 2b. In contrast to the fluorescence image, the differential $\mathrm{Im}\{\Delta_p - \Delta_s\}$ image reveals hybridization in both column 1 (*label-free*) and column 3 (Cy5-labeled) with almost equal contrast.

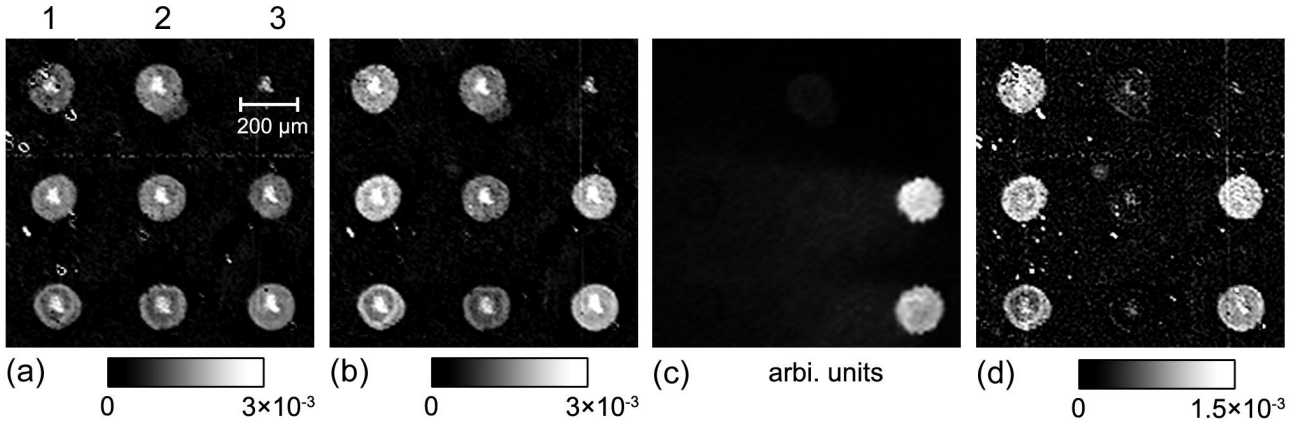

Fig. 2 OI-RD and fluorescence scans of a microarray of 60-base oligonucleotides before and after hybridization. Columns 1, 2, and 3 are printed with different oligonucleotides. The top position in column 3 is left blank for alignment. (a) $\mathrm{Im}\{\Delta_p - \Delta_s\}$ image of the printed microarray before hybridization; (b) $\mathrm{Im}\{\Delta_p - \Delta_s\}$ image of the microarray after hybridization with unlabeled oligonucleotide complementary to column 1 and Cy5-labeled oligonucleotide complementary to column 3; (c) Cy5 fluorescence image after hybridization; (d) Differential $\mathrm{Im}\{\Delta_p - \Delta_s\}$ image obtained by subtracting Fig. 2a from Fig. 2b, revealing hybridized spots in both column 1 (*label-free*) and column 3 (Cy5-labeled).

4.2. Optical properties of dry oligonucleotide films

We now present a quantitative analysis of the optical signal using Eq. (1) to determine the thickness of the oligonucleotides on the microarray before and after hybridization. In Fig. 3a we plot the spatially averaged $\mathrm{Im}\{\Delta_p - \Delta_s\}$ over the printed spot area (after 60 mJ/cm^2 UV irradiation and removal of the excess unbound oligonucleotides) vs. printing concentration. Each point is the mean of four replicate spots printed at separate locations on the microarray and

the error bars are the standard deviations. $\mathrm{Im}\{\Delta_p-\Delta_s\}$ levels off to 2.0×10^{-3} for all spots printed with concentrations in excess of 40 ~ 50 μM, indicating that a stably bound monolayer of oligonucleotides forms on the poly-L-lysine coated glass slide with a density near *saturation*. The error bars in Fig. 3a show the variation in $\mathrm{Im}\{\Delta_p-\Delta_s\}$ among spots that were printed at the same concentration. The actual detection limit of our current microscope is at least one order of magnitude smaller than the smallest error bar shown. Near the saturation density, the dielectric constant of the oligonucleotide monolayer[11] is expected to be $\varepsilon_d = 2.14$. Using Eq. (1) with $\theta = 45^o$ and $\varepsilon_d = 2.14$, we find that the thickness of the unlabeled oligonucleotide monolayer *before* hybridization is 1.2 nm, very close to the diameter of a single stranded oligonucleotide. This means that the 60-base oligonucleotides lay more or less flat on the substrate[8] at this level of UV cross-linking. After hybridization (see Fig. 2d), assuming the molecular density remains constant, the increase in $\mathrm{Im}\{\Delta_p-\Delta_s\}$ by 1.0×10^{-3}, corresponds to a change of 0.6 nm in thickness. Since the printed film inevitably contains sterically inaccessible oligonucleotides, due to entanglement or cross-linking for example, a film thickness change less than 1 nm after a "nearly complete" hybridization is expected. Fig. 3b demonstrates the effect that UV irradiation has upon the retention of oligonucleotides after the post-printing wash. The microarray irradiated at 60 mJ/cm^2 saturates with a thickness of 1.2 nm as before, while the microarray irradiated at 600 mJ/cm^2 saturates at about 2.8 nm. This increased thickness indicates that the oligonucleotides no longer lay flat since the parts of the oligonucleotides not cross-linked to the substrate are free to stretch in the direction perpendicular to the substrate.

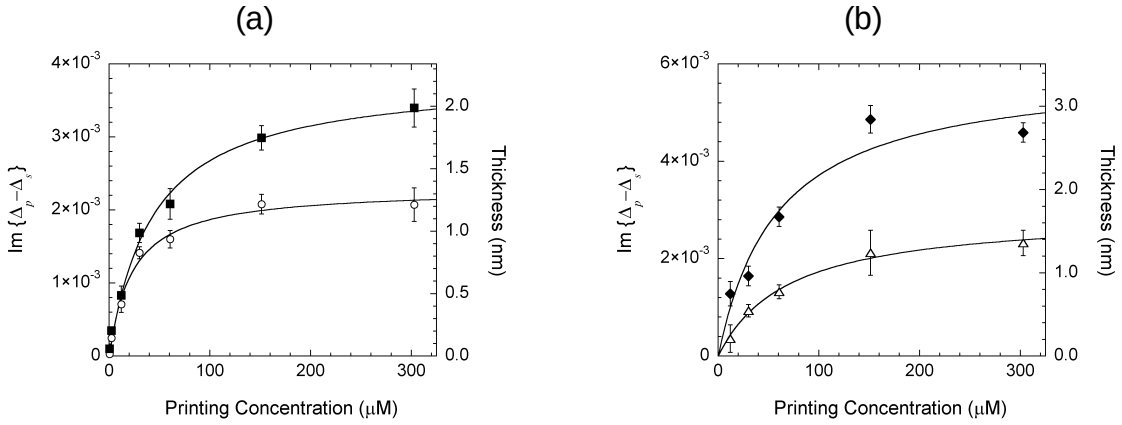

Fig. 3 $\mathrm{Im}\{\Delta_p-\Delta_s\}$ averaged over the area of a printed oligonucleotide spot vs. printing concentration. (a) Effect of hybridization on a microarray after 60 mJ/cm^2 UV cross-linking and washing. Open circles: before hybridization (after washing). Solid squares: after hybridization. (b) Effect of UV irradiation on retention of oligonucleotides after washing. Open triangles: 60 mJ/cm^2. Solid diamonds: 600 mJ/cm^2. The curves in Figs. 3a and 3b and are guides for the eyes.

4.3. Optical properties of wet oligonucleotide films

Next we present a quantitative analysis of the optical signal of oligonucleotide films immersed in water. Fig. 4a is an image of a dry oligonucleotide microarray acquired in the configuration of Fig. 1a with $\theta = 60^o$. The microarray was UV cross-linked at 600 mJ/cm^2 and washed to remove excess oligonucleotides. Fig. 4b is an image of the same dry microarray, but acquired in the configuration of Fig. 1b with $\theta = 34.7^o$. The resolution of the image has decreased because we have not yet compensated for the aberrations induced in the beam by passing through the transparent substrate at oblique incidence. Fig. 4c is like Fig. 4b except now the reaction chamber has been filled with water so that the microarray is completely immersed. This image demonstrates that OI-RD can be effectively used to detect microarrays *in-situ.* Furthermore, since images of the microarray in two different ambient media were acquired, Eqs. (1) and (2) can be used to determine *both* the dielectric constant and thickness of the film. To accomplish this, we assume that the thickness of the films are the same when wet or dry, but we allow the dielectric constant to be different for wet and dry films. The spatially averaged dielectric constants and film thicknesses are obtained by minimizing an error function defined as

$$F\left(\varepsilon_{\text{Dry DNA}}, \varepsilon_{\text{Wet DNA}}, d_1, d_2, d_3\right) = \sum_i \left[\text{Im}\left\{\Delta_p - \Delta_s\right\}_{\text{Calc}} - \text{Im}\left\{\Delta_p - \Delta_s\right\}_{\text{Meas}} \right]^2, \quad (3)$$

where $\varepsilon_{\text{Dry DNA}}$ and $\varepsilon_{\text{Wet DNA}}$ are the dielectric constants of the dry and wet oligonucleotide films, respectively, d_1 , d_2, and d_3 are the spatially averaged thicknesses of the spots from least to most concentrated, $\text{Im}\{\Delta_p - \Delta_s\}_{\text{Meas}}$ is the spatially averaged OI-RD signal for each spot in Figs. 4a-c, and $\text{Im}\{\Delta_p - \Delta_s\}_{\text{Calc}}$ is the theoretical expression for the signal obtained from Eqs. (1) or (2) as appropriate. The values obtained by this process are $\varepsilon_{\text{Dry DNA}} = 2.05$, $\varepsilon_{\text{Wet DNA}} = 1.90$, $d_1 = 1.4$ nm, $d_2 = 2.0$ nm, and $d_3 = 3.2$ nm. The value obtained for $\varepsilon_{\text{Dry DNA}}$ is reasonably close to the previously assumed value of 2.14. Furthermore, the smaller value of $\varepsilon_{\text{Wet DNA}}$ is expected since the dielectric constant of the hydrated film can be thought of as an effective mixture of the dielectric constant of the dry oligonucleotide and the water.

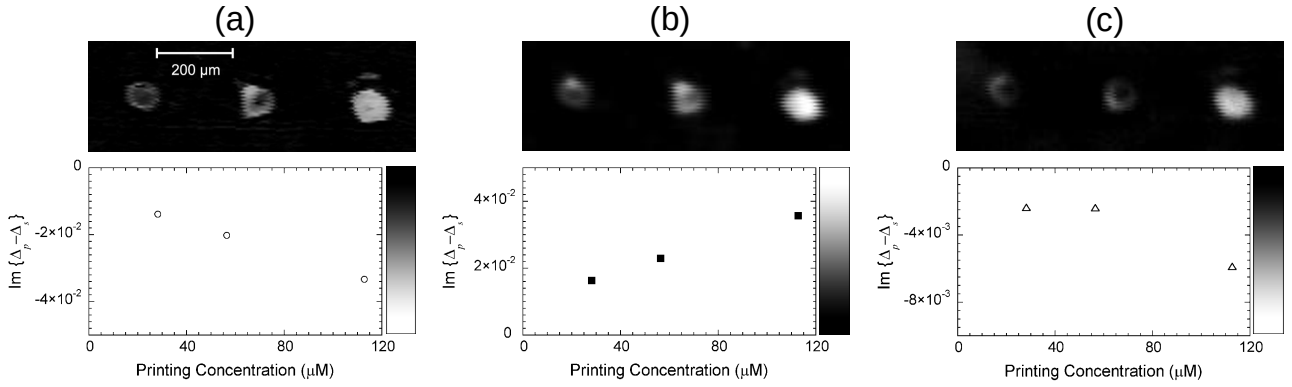

Fig. 4 (a) $\text{Im}\{\Delta_p - \Delta_s\}$ image of a dry oligonucleotide microarray with the OI-RD microscope in the configuration shown in Fig. 1a. The plot shows $\text{Im}\{\Delta_p - \Delta_s\}$ averaged over the area of each spot and indicates the intensity scale used in the image. (b) $\text{Im}\{\Delta_p - \Delta_s\}$ image of the dry microarray with the OI-RD microscope in the configuration shown in Fig. 1b (reaction chamber empty). (c) $\text{Im}\{\Delta_p - \Delta_s\}$ image of the wet microarray with the OI-RD microscope in the configuration shown in Fig. 1b (reaction chamber filled with ddH_2O).

4.4. OI-RD and fluorescence detection of IgG microarrays

Figure 5(a) shows $\text{Im}\{\Delta_p - \Delta_s\}$ for an IgG protein microarray printed on aldehyde-derivatized glass and Figure 5(b) is a corresponding two-color fluorescence image (Cy3 and Cy5 fluorescence). Rabbit, mouse, and human IgG solutions were printed in a series of concentrations. The nominally labeled IgG solutions were actually a mixture of approximately equal parts labeled and unlabeled IgG. The images in Figures 5(a) and 5(b) were acquired after removing excess printed protein as described previously. The OI-RD image shows both the labeled and unlabeled IgG films covering the printed spots. However, the fluorescence image reveals that the Cy5 and Cy3 labeled IgG proteins tend to aggregate together, in this case on the edge of the printed spot. Since the OI-RD image reveals the presence of a film in the center of these spots, we conclude that this film must be the unlabeled IgG printed on the same spot. During printing the solid pin makes contact with the substrate, which tends to squeeze solution to the edge of the pin. Furthermore, solid printing pins also have a tendency to remove liquid from the center of the deposited droplet during the upstroke of the pin[1]. Figs. 5a and 5b suggest that the labeled IgG molecules remain on the edge of the spot after printing while the unlabeled IgG wets the entire spot. This difference in wetting behavior is likely due to the hydrophobicity of the cyanine dye labels. These observations illustrate the potentially undesirable impact labeling can have upon the physical properties of proteins on microarrays.

To confirm the presence of unlabeled IgG in the center of the spots, the microarray was blocked with IgG-free BSA and then reacted with Cy3 labeled goat anti-human secondary antibody. The region of interest for the reaction is boxed in Figures 5(a) and 5(b). Cy3 fluorescence images of the region of interest before and after reaction with the fluorescent secondary antibody are given in Figures 5(c) and 5(d). The reaction with the HM column revealed that the unlabeled human IgG covered the entire spot and did not aggregate on the edge. The reaction with the HM5 column

showed that the secondary antibody reacted with the labeled IgG on the edge of the spot and with unlabeled IgG in the center of the spot, consistent with the OI-RD image.

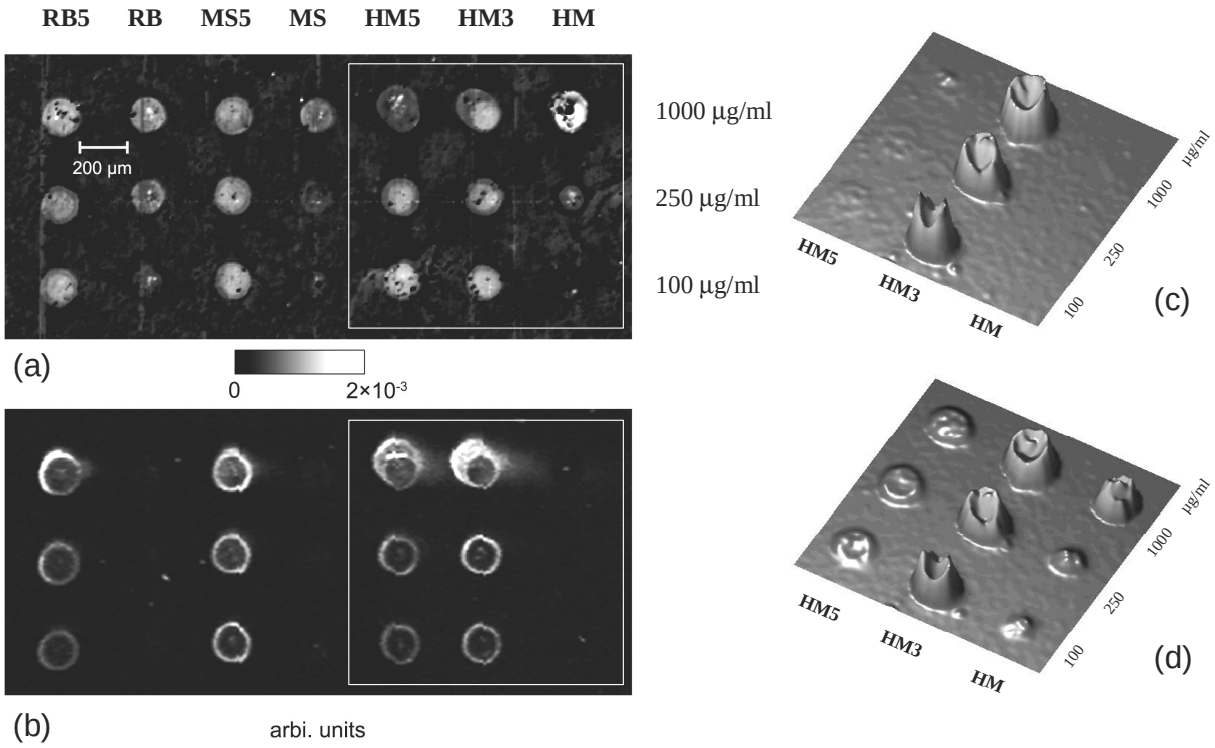

Fig. 5 (a) Im{$\Delta_p - \Delta_s$} image of an IgG protein microarray. Rabbit IgG (RB), Cy5 labeled rabbit IgG (RB5), mouse IgG (MS), Cy5 labeled mouse IgG (MS5), human IgG (HM), Cy3 labeled human IgG (HM3), and Cy5 labeled human IgG (HM5) were printed in a series of concentrations (listed on the right). (b) Combined Cy3 and Cy5 fluorescence image of the IgG microarray. Cy3 fluorescence images of region of interest (boxed in Fig. 5a and Fig. 5b) (c) before reaction and (d) after reaction with Cy3 labeled goat anti-human antibody.

5. DISCUSSION

Other label-free methods exist for microarray detection, most notably surface plasmon resonance microscopy (SPR)[12] and mass spectrometry[13]. Mass spectrometry requires that microarrays are fabricated on a special matrix medium for laser-induced desorption and ionization. The sensitivity of SPM derives from the sharp resonance of plasmon surface polariton and thus requires microarrays to be fabricated on functionalized gold films. In comparison, the OI-RD microscope only requires optically flat substrates. This gives flexibility in the choice of immobilization chemistry used in microarray fabrication. For example, we have used chemically modified glass substrates that are in widespread use for fluorescence-detection of microarrays. The present scanning OI-RD microscope can also be configured into a non-scanning microscope by using 2D detectors such as CCD. Furthermore, similar to SPR, the OI-RD microscope is an *in-situ* detection method allowing high-throughput parallel assays of biochemical kinetics and noninvasive imaging of microarrays at intermediate processing steps.

6. CONCLUSION

We have demonstrated that an OI-RD microscope can quantitatively detect microarrays of biological macromolecules without labeling. Such a microscope is particularly useful in investigations of biochemical processes on microarrays that may be adversely influenced by labeling agents. Furthermore, the non-invasive and *in situ* aspects

of an OI-RD microscope enable it to be used for high throughput assays of biomolecular kinetics as well as quality control of microarray fabrication and processing.

Table 1. Sequences of printed oligonucleotides

Column 1	5'-TCACAAACCC GTCCTACTCT ACTAGCTGCA GTAGCCCCAC TGGTTCCCGT TTCCGATGTT-3'
Column 2	5'-CCTTGTACCG CTGAGTTCAC ACCGACACAC CTCACCACAC TTACACCGTC CACAAAGAGA-3'
Column 3	5'-TTTCCATGCG GACCTACCAC CGTAGTACCT CGCAATGCCA GTGCAACAAG TACACCTGGA-3'

ACKNOWLEDGEMENTS

This work was supported by National Science Foundation under NSF-DMR-9818483, and in part by the NSF Center for Biophotonics Science & Technology, managed by the University of California at Davis, under Cooperative Agreement No. PHY0120999.

REFERENCES

1. Mark Schena, Microarray Analysis, 1-17, 114-117, 184, John Wiley and Sons, Hoboken, 2003.
2. G. MacBeath, "Protein microarrays and proteomics", *Nature Genet*. **32**, 526-532, 2002.
3. P. Mitchell, "A perspective on protein microarrays", *Nature Biotech*. **20**, 225-229, 2002.
4. A. Wong and X. D. Zhu, "An optical differential reflectance study of adsorption and desorption of xenon and deuterium on Ni(111)", *Appl. Phys. A* **63**, 1-8, 1996.
5. X. D. Zhu, H. B. Lu, Y. Guo-Zhen, L. Zhi-Yuan, G. Ben-Yuan, Z. Dao-Zhong, "Epitaxial growth of $SrTiO_3$, on $SrTiO_3$(001) using an oblique-incidence reflectance-difference technique", *Phys. Rev. B* **57**, 2514-2519, 1998.
6. R. M. A. Azzam and N. M. Bashara, *Ellipsometry and Polarized Light*, 305-306, Elsevier Science, New York, 1987.
7. J. Gray, P. Thomas, X. D. Zhu, "Laser pointing stability measured by an oblique-incidence optical transmittance difference technique", *Rev. Sci. Instru.* **72**, 3714-3717, 2001.
8. S. V. Lemeshko, T. Powdrill, Y. Y. Belosludtsev, M. Hogan, "Oligonucleotides form a duplex with non-helical properties on a positively charged surface", *Nucleic Acids Res*. **29**, 3051-3058, 2001.
9. M. D. Eisen and P. O. Brown, "DNA arrays for analysis of gene expression", *Methods in Enzymology* **303**, 179-205, 1999.
10. H. J. Gruber, C. D. Hahn, G. Kada, C. K. Riener, G. S. Harms, W. Ahrer, T. G. Dax, H. G. Knaus, "Anomalous fluorescence enhancement of Cy3 and Cy3.5 versus anomalous fluorescence loss of Cy5 and Cy7 upon covalent linking to IgG and noncovalent binding to avidin", *Bioconjugate Chem*. **11**, 696-704, 2000.
11. D. E. Gray, S. C. Case-Green, T. S. Fell, P. J. Dobson, E. M. Southern, "Ellipsometric and interferometric characterization of DNA probes immobilized on a combinatorial array", *Langmuir* **13**, 2833-2842, 1997.
12. J. M. Brockman, B. P. Nelson, R. M. Corn, "Surface plasmon resonance imaging measurements of ultrathin organic films", *Ann. Rev. Phys. Chem*. **51**, 41-63, 2000.
13. E. Scrivener, R. Barry, A. Platt, R. Calvert, G. Masih, P. Hextall, M. Soloviev, J. Terrett, "Peptidomics: A new approach to affinity protein microarrays", *Proteomics* **3**, 122-128, 2003.